



Published in final edited form as:

*Analyst*. 2016 April 7; 141(7): 2278–2283. doi:10.1039/c5an02656c.

## Sensitive magnetic nanoparticle-based immunoassay of phosphorylated acetylcholinesterase using protein cage templated lead phosphate for signal amplification with graphite furnace atomic absorption spectrometry detection

Pei Liang<sup>a,\*</sup>, Caiyan Kang<sup>a</sup>, Enjian Yang<sup>a</sup>, Xiaoxiao Ge<sup>b</sup>, Dan Du<sup>b,\*</sup>, and Yuehe Lin<sup>b</sup>

<sup>a</sup> Key Laboratory of Pesticide & Chemical Biology of Ministry of Education, College of Chemistry, Central China Normal University, Wuhan 430079, P. R. China

<sup>b</sup> School of Mechanical and Materials Engineering, PO Box 642920; Washington State University, Pullman, WA 99164, USA

### Abstract

We developed a new magnetic nanoparticles sandwich-like immunoassay using protein cage nanoparticles (PCN) for signal amplification together with graphite furnace atomic absorption spectrometry (GFAAS) for quantification of organophosphorylated acetylcholinesterase adduct (OP-AChE), the biomarker of exposure to organophosphate pesticides (OPs) and nerve agents. OP-AChE adducts were firstly captured by titanium dioxide coated magnetic nanoparticles (TiO<sub>2</sub>-MNPs) from the sample matrixes through metal chelation with phospho-moieties, and then selectively recognized by anti-AChE antibody labeled on PCN which was packed with lead phosphate in its cavity (PCN-anti-AChE). The sandwich-like immunoreaction was performed among TiO<sub>2</sub>-MNPs, OP-AChE and PCN-anti-AChE to form TiO<sub>2</sub>-MNPs/OP-AChE/PCN-anti-AChE immunocomplex. The complex could be easily isolated from the sample solution with the help of magnet, and the released lead ions from PCN were detected by GFAAS for the quantification of OP-AChE. Greatly enhanced sensitivity was achieved because PCN increased the amount of metal ions in the cavity of each apoferritin. The proposed immunoassay yielded a linear response over a broad OP-AChE concentrations from 0.01 nM to 2 nM, with a detection limit of 2 pM, which has enough sensitivity for monitoring of low-dose exposure to OPs. This new method showed an acceptable stability and reproducibility and was validated with OP-AChE spiked human plasma.

### Keywords

Protein cage; amplification; phosphorylated acetylcholinesterase; magnetic nanoparticles; immunoassay; graphite furnace atomic absorption spectrometry

---

\* Corresponding author. liangpei@mail.ccn.u.edu.cn; annie.du@wsu.edu.

## Introduction

Many organophosphates (OPs) have been extensively used in agriculture as insecticides or acaricides.<sup>1</sup> As a result, OPs contaminations have been widespread in air, water, soil and food, and there is a potential for human exposure. Exposure to even small amounts of OPs can be fatal because they exert their toxicity through irreversible phosphorylation and inactivation of acetylcholinesterase (AChE) in the central nervous system, often leading to perturbation of the nerve conduction system and to the rapid paralysis of vital functions of living systems.<sup>2,3</sup> Thus, developing a simple, rapid, sensitive and reliable method for monitoring of OPs exposure and screening poison victims is desired.

OPs exposure will produce numbers of relevant biomarkers in biological system, including phosphorylated enzyme adducts, hydrolysis products and unbound free OPs.<sup>4,5</sup> Detection of metabolites and free OPs could be performed by gas chromatography-mass spectrometry (GC-MS) or liquid chromatography-mass spectrometry (LC-MS), but these methods are not accurate due to the high affinity of OPs to cholinesterase (ChE) and other proteins.<sup>6,7</sup> Phosphorylated ChE adduct (OP-ChE) is a more effective and sensitive biomarker for directly evaluation of OPs exposure in the absence of baseline.<sup>8</sup> Clinical measurement of OP-ChE adducts biomarker shows great promise for early predictions. Although GC-MS and LC-MS are powerful tools for the detection of OP-ChE adducts, they have some inherent disadvantages such as complicated and expensive analysis, and lack of portability and real-time results.<sup>9</sup>

Immunoassay of OP-ChE adducts is an optional technology with high sensitivity and selectivity. Combined with nanomaterial labels based signal amplification strategies, immunoassay have attracted considerable interest and are extensively applied in the determination of proteins because of their low-background signal, high signal to noise ratio, low cost, long lifetime, inherent miniaturization and multiplexing capability.<sup>10,11</sup> The nanomaterials used in immunoassay include metal nanoparticles (gold, silver),<sup>12,13</sup> semiconductor nanoparticles (quantum dots)<sup>14,15</sup> and markers loaded nanocarriers (carbon nanotubes, apoferritin, silica nanoparticles, and liposome beads).<sup>16</sup> Antibodies (antigens) labeled with nanomaterials could retain their bioactivity and interact with their counterparts. Quantification is generally achieved by measuring the specific signal of a nanomaterial label after immunoreaction. Issues to be considered with nanomaterial labels include the difficulty of making uniformly sized metal nanoparticles and the unstable nature of the linkage between the nanoparticles and the proteins.<sup>17</sup> Apoferritin-templated nanoparticles overcome all of these limitations. Apoferritin, a typical protein cage, is an iron storage protein with a diameter of 12.5 nm.<sup>18</sup> It has a cavity of 8 nm in diameter, surrounded by 24 polypeptide subunits, which can store up to 4500 iron atoms in its fully saturated form; however, it more commonly holds 2000 iron atoms per apoferritin in the iron phosphate form. There are 6 hydrophobic channels and 8 hydrophilic channels connecting the outside of apoferritin with its interior. 8 hydrophilic channels facilitate the passage of metal ions and small molecules into the cavity of the protein.<sup>19,20</sup> Due to the center cavity structure as well as the dissociation and reconstructive characteristics of apoferritin at different pH environments, it provides a restrained environment to produce encoded nanoparticle tags with uniformly size, and the labels are compatible with biomolecules due to the protein cage.<sup>21,22</sup> We have

taken the advantages of apoferritin to synthesize inorganic nanoparticles as labels for the electrochemical immunoassay of DNA and protein, and confirmed the stability and the specific binding with antigen of the apoferritin-labeled antibody. Highly sensitivity could be easily obtained due to the large quantities of detectable metal ions in the cavity of each apoferritin.<sup>23-25</sup> Nevertheless, there was no report on apoferritin-labeled immunoassay followed by atomic spectrometry detection until now.

Immunoassay detection of OP-ChE is a highly sensitive method with high selectivity, but sometimes challenged with unavailability of OP-specific antibodies. To help address this issue, zirconia or titania nanoparticles ( $ZrO_2$  or  $TiO_2$  NPs) were performed as the selective sorbents to recognize the phosphorylation moiety based on the strong chelation with phospho-moieties.<sup>26, 27</sup> Magnetic titania nanoparticles was synthesized (composite of  $Fe_3O_4$ ,  $SiO_2$ , and  $TiO_2$ ) with an aim to combine the magnetic property of magnetite particles and affinity of  $TiO_2$  toward phosphopeptides for fast enrichment of phosphopeptides.<sup>28</sup>  $TiO_2$  or  $ZrO_2$  NPs could be used as a special “similar antibodies” because of its specific capture phosphate group in OP-ChE and good biocompatibility.<sup>29, 30</sup>

In this paper, we demonstrated a novel magnetic nanoparticles based immunoassay for highly selective and sensitive detection of OP-ChE adducts in human plasma using apoferritin encoded metallic tags in the signal amplification strategy. Phosphorylated acetylcholinesterase (OP-AChE) was prepared by incubating AChE with paraoxon, which was used as the model target in this study. OP-AChE adducts were captured by titanium dioxide coated magnetic nanoparticles ( $TiO_2$ -MNPs) from the sample matrixes through metal chelation with phospho-moieties, and then selectively recognized by anti-AChE antibody labeled on protein cage nanoparticles (PCN) which was packed with lead phosphate (PCN-anti-AChE) to form a sandwich-like immunocomplex. The complex could be easily isolated from the sample solution with the help of magnet, and dissolved in  $HNO_3$  solution to release the lead ion which were detected by graphite furnace atomic absorption spectrometry (GFAAS) for the quantification of OP-AChE. The use of  $TiO_2$ -MNPs not only surpasses the drawback of the scarce commercial availability of OP-specific antibody, but also favors the separation of the immunocomplex from the sample matrixes.

## Experimental

### Apparatus

A TAS-990 atomic absorption spectrophotometer (Beijing Purkinge General Instrument Co. Ltd., Beijing, China) with a deuterium back-ground correction and a GF990 graphite furnace atomizer system was used for the determination of Pb. A lead hollow-cathode lamp was used as radiation source at 283.3 nm. The optimum operating parameters for GFAAS are given in Table 1. All measurements were carried out in the integrated absorbance (peak area) mode. Attenuated total reflection Fourier-transform infrared spectra (ATR-FTIR) were recorded on a Nexus 470 FTIR (Nicolet, USA) equipped with an omni sampler over 32 scans, which was used to characterize the formation of OP-AChE adduct.

## Reagents and materials

Anti-AChE antibody was purchased from Abcam Inc. (Cambridge, MA). Apoferritin, human AChE, paraoxon, avidin, biotin N-hydroxysuccinimide (biotin-NHS), bovine serum albumin (BSA), phosphate buffer saline (PBS), Tris-HCl buffer were purchased from Sigma-Aldrich Co. (St. Louis, MO). SuperBlock T20 (TBS) blocking buffer and Bicinchoninic acid assay (BCA) kit were purchased from Thermo scientific (Rockford, IL). Tween-20, lead nitrate (AR) were purchased from Shanghai Chemistry Reagent Company (Shanghai, China). TiO<sub>2</sub>-MNPs were synthesized by hydrolysis of tetrabutyltitanate on the surface of Fe<sub>3</sub>O<sub>4</sub> magnetic nanospheres, and characterized by ATR-FTIR, transmission electron microscope and X-ray diffraction as previously described elsewhere.<sup>31</sup> All stock and buffer solutions were prepared with double distilled water.

## Preparation of OP-AChE adduct

OP-AChE was by mixing 50  $\mu\text{L}$  AChE ( $500 \text{ nmol L}^{-1}$ ) and 100  $\mu\text{L}$  paraoxon ( $750 \mu\text{mol L}^{-1}$ ) in double distilled water and incubated at room temperature for 12 h. The enzyme activity was determined with *Ellman assay*<sup>32</sup> until AChE was completely inhibited by paraoxon. The resulting solution was then exhaustively dialyzed with  $0.01 \text{ mol L}^{-1}$  Tris-HCl buffer solution (pH 8.0) for 72 h to remove unbound paraoxon and the outcome p-nitrophenoxy. Moreover, the resultant OP-AChE was concentrated with ultrafiltration to a final volume of 1.0 mL and stored at  $-20 \text{ }^\circ\text{C}$  for the future using. The protein concentrations of the OP-AChE stock solution were determined to be  $6.8 \mu\text{mol L}^{-1}$  by BCA method.<sup>33</sup> The working solutions of OP-AChE were obtained by appropriate dilution of the stock solution with Tris-HCl buffer in the following experiment.

## Preparation of lead phosphate packed PCN

Lead phosphate packed PCN was prepared according to our previous method.<sup>21</sup> Briefly, 40  $\mu\text{L}$  apoferritin ( $50 \text{ mg mL}^{-1}$ ) was diluted with Tris-HCl ( $0.1 \text{ mol L}^{-1}$ , pH 8.0) to a volume of 1.5 mL in EP tube. Approximately 250  $\mu\text{L}$  of  $6 \text{ mmol L}^{-1}$  lead nitrate was slowly introduced into the above apoferritin solution, and the mixture was continuously stirred for 1 h to allow the lead ions to diffuse into the cavity of apoferritin. Then 250  $\mu\text{L}$  PBS ( $0.2 \text{ mol L}^{-1}$ , pH 7.0) was drop-by-drop added into the solution and the mixture was stirred for 1 h to form the metal phosphate core inside apoferritin. Excess lead ions remaining outside the apoferritin were precipitated with PBS buffer. The mixture was centrifuged at 5000 rpm for 5 min. The supernatant was washed three times with  $0.1 \text{ mol L}^{-1}$  Tris-HCl using an ultrafiltration (10 KD), and reconstituted to a final volume of 1.0 mL. The concentrations of apoferritin and Pb ion were determined by the BCA method and GFAAS, respectively. The numbers of Pb ion loaded in apoferritin, calculated by comparing the concentrations of apoferritin and Pb ion in the nanoparticle solution, are estimated to be 1400 per apoferritin.

## Preparation of PCN-anti-AChE conjugate

The PCN-anti-AChE was prepared using an avidin as a bridge to link biotin modified anti-AChE and apoferritin.<sup>34</sup> In this procedure, biotin labeled PCN (biotin-PCN) and biotin labeled anti-AChE (biotin-anti-AChE) were first prepared, respectively. And then native unlabeled avidin was used to connect both of them since avidin possesses 4 active sites

which will react with one biotin residue and operate as acceptor for another biotin-labeled protein. Briefly, 800  $\mu\text{L}$  of the above prepared PCN nanoparticles were mixed with 200  $\mu\text{L}$  0.1  $\text{mg mL}^{-1}$  biotin-NHS and stirred for 3 h at room temperature. The mixture was dialyzed against Tris-HCl overnight to remove excess biotin-NHS. The resulting biotin-PCN was reconstituted into a 1.0 mL solution containing 0.5% BSA and stored at 4  $^{\circ}\text{C}$ . The same process was performed to prepare the biotin-anti-AChE. Subsequently, 1.0 mL 0.06  $\text{mg mL}^{-1}$  avidin was mixed with the above biotin-PCN and reacted for 2 h to form avidin-biotin-PCN conjugate. Then an amount of biotin-anti-AChE was added at an equal molar equivalent to the avidin-biotin-LPA solution, and the reaction proceeded for 2 h to form PCN-biotin-avidin-biotin-anti-AChE (PCN-anti-AChE) conjugate. Excess agents were removed using an ultrafiltration (10 KD). The resulting PCN-anti-AChE was dispersed in Tris-HCl buffer containing 1% BSA and kept at 4  $^{\circ}\text{C}$  for the further using.

### Immunoassay procedure

A sandwich-like immunoassay shown in figure 1 was used for the determination of OP-AChE. A certain amount of  $\text{TiO}_2$ -MNPs were dispersed by ultrasound in acetate buffer (pH 4.0) to a concentration of 0.5% (w/v), and 25  $\mu\text{L}$  aliquot of  $\text{TiO}_2$ -MNPs was transferred into 1.5 mL EP tube. Then, 25  $\mu\text{L}$  aliquot of OP-AChE or spiked samples, which was diluted to the desired concentration with acetate buffer containing 0.5% BSA, was introduced into the EP tube and vortexed for 30 min at room temperature. The mixtures were washed intensively with Tris-HCl buffer and blocked with TBS blocking buffer for 30 min in order to reduce nonspecific binding. After magnetically separated and re-dispersed in acetate buffer, 10  $\mu\text{L}$  of PCN-anti-AChE conjugate was added, and the incubation of 40 min with gentle shaking results in a sandwich immunocomplex ( $\text{TiO}_2$ -MNPs/OP-AChE/PCN-anti-AChE). After rinsing with Tris-HCl buffer thoroughly and magnetic separation, the complex attached on the tube wall. 20  $\mu\text{L}$  of 1.0  $\text{mol L}^{-1}$   $\text{HNO}_3$  solution was added into the tube and mixed with the complex for 5 min to release Pb from PCN, and then diluted to 100  $\mu\text{L}$  with double distilled water. 10  $\mu\text{L}$  of the solution was injected into GFAAS for the determination of Pb.

## Result and Discussion

### Characterization of OP-AChE by ATR-FTIR

In this study, OP-AChE adduct was prepared by incubating AChE with paraoxon, and used as a model of OP-AChE. FTIR spectra of OP-AChE were recorded to confirm the formation of phosphorylated AChE adduct. As shown in figure 2. Strong bands resulting from O-C-C stretching (1043 and 931  $\text{cm}^{-1}$ ) are exhibited in the spectra of OP-AChE, while some bands associated with conjugated double bonds (1611, 1595, 1525 and 1490  $\text{cm}^{-1}$ ) and aryl- $\text{NO}_2$  (1349, 1286 and 861  $\text{cm}^{-1}$ ) in the spectra of paraoxon was absent. These results consistent with the understanding that the phosphorylation of AChE by paraoxon is synchronous with the release of p-nitrophenoxy ( $-\text{OPhNO}_2$ ) to yield a stable, covalent diethylphosphoserine ester bond.

### Evaluation of immunoaffinities between $\text{TiO}_2$ -MNPs, antibody and OP-AChE

The immunoaffinities of  $\text{TiO}_2$ -MNPs, OP-AChE and PCN-anti-AChE antibody were studied by GFAAS measurements. Here, 1.0 nM nonphosphorylated AChE, 1.0 nM paraoxon and

1% BSA were served as the control samples to be simultaneously examined as the challenging proteins, and the results were shown in figure 3. It can be seen that the absorbance signal for OP-AChE is much higher than that for nonphosphorylated AChE, paraoxon and BSA, indicating the effective immunoreactions between TiO<sub>2</sub>-MNPs, OP-AChE and PCN-anti-AChE to form the sandwich-like immunocomplex. The absorbance signals from these control samples might be ascribed to the nonspecific adsorption of PCN-anti-AChE to the TiO<sub>2</sub>-MNPs.

### Optimization of detection conditions for OP-AChE

In this work, TiO<sub>2</sub>-MNPs is used as “similar antibodies” for the trapping of OP-AChE, its amount influenced the amount of captured OP-AChE which accounted for the amount of PCN-anti-AChE. The effect of the amount of TiO<sub>2</sub>-MNPs on the Immunoassay was studied through varying the concentration of TiO<sub>2</sub>-MNPs dispersion from 0.1% to 1% (w/v), and the results were shown in figure 4. As can be seen, the absorbance signal of Pb increased quickly with the increasing of TiO<sub>2</sub>-MNPs concentration from 0.1% to 0.5%, and increased slightly after 0.5%. In the other hand, excessive TiO<sub>2</sub>-MNPs may cause the nonspecific adsorption and influence on the Immunoassay response. So 0.5% TiO<sub>2</sub>-MNPs dispersion was used in the experiments.

Acidity is another important issue for the capturing of OP-AChE by TiO<sub>2</sub>-MNPs. As reported in literature, TiO<sub>2</sub> is an amphoteric oxide that can react either as Lewis acid or base depending on the pH of the solution.<sup>35</sup> Under acidic conditions, TiO<sub>2</sub> with positively charged titanium atoms (Lewis acid) shows high binding affinity to phosphate ion (Lewis base), suggesting that high binding selectivity to phosphorylated protein could be achieved. In this work, it was found that the highest absorbance signal of Pb was achieved at pH 4.0. Lower acidity does not mean the best condition since phosphate ions may be prone to bind with hydrogen ions, and the protein may be damaged. Therefore, pH 4.0 was selected for the capturing of OP-AChE.

The incubation time is one of the important parameters for both TiO<sub>2</sub>-MNPs capturing of OP-AChE and PCN-anti-AChE recognition of the captured OP-AChE. As shown in figure 5, the absorbance signal of Pb increased with the increasing incubation time and tend to a steady value after 30 min (TiO<sub>2</sub>-MNPs capturing) and 40 min (PCN-anti-AChE recognition), respectively, which were selected for TiO<sub>2</sub>-MNPs capturing and PCN-anti-AChE recognition of OP-AChE in the sandwich immunoassay. Longer incubation time could result in a large non-specific signal.

Nonspecific adsorption has a significant influence on the immunoassay response. As can be seen in figure 6, obviously negligible signal was observed when using 0 nM OP-AChE and 5.0 nM nonphosphorylated AChE as the control sample without blocking. To minimize nonspecific adsorption, TBS buffer was used as the blocking agent and 1% BSA was added to the synthesized PCN-anti-AChE conjugate. Although both the absorbance signals of the OP-AChE sample and the control sample decreased after blocking due to the shield effect of the blocking agent, the single-to-noise was improved greatly.

For GFAAS determination of Pb after the immunoreaction, a pyrolysis step prior to the atomization is needed to remove the matrix as much as possible which could considerably reduce the magnitude of the background signal. In order to avoid Pb losing during the pyrolysis step and obtain the high absorbance signal, the optimal pyrolysis and atomization temperatures should be selected. Pyrolysis and atomization curves were established using the solution obtained after the immunoassay procedure, and shown in figure 7. From the curves, 500 °C and 1700 °C were selected as the optimal pyrolysis and atomization temperatures, respectively.

### Analytical performance of the immunoassay

Under optimal experimental conditions, the proposed immunoassay was examined with different concentrations of OP-AChE. A well-defined absorbance signal from lead ion was observed and increased with the increase of OP-AChE concentration. The resulting calibration plot of absorbance signal vs. concentration was linear over 0.01-2 nM OP-AChE with a correlation of 0.9995. The limit of detection (LOD), based on a signal-to-noise ratio (S/N) of 3, was 2 pM. Since the average AChE concentrations in human plasma and erythrocyte are around 0.12 nM and 3 nM respectively, the proposed immunoassay has enough sensitivity for monitoring of low-dose exposure to OPs. Such a detection limit is comparable to that of mass spectrometry analysis of organophosphorylated cholinesterase adducts (1.0~4.0 ng mL<sup>-1</sup>),<sup>8</sup> and 10 times lower than our previous result of 0.02 nM adducts using the electrochemical detection.<sup>24</sup> The precision of the proposed method was evaluated by analyzing one sample for six replicate determinations, and the coefficients of variation (CV) was 4.6% at 0.1 nM OP-AChE level.

A series of OP-AChE human plasma samples were used to investigate the accuracy and practical viability of the proposed immunoassay. The OP-AChE human plasma samples were prepared by spiking different amounts of OP-AChE with known concentration to human plasma. Each sample was determined three times, and the results were summarized in Table 2. The recoveries were in the range of 94-105%, indicating that the magnetic nanoparticles based immunoassay was reliable.

### Supplementary Material

Refer to Web version on PubMed Central for supplementary material.

### Acknowledgment

We acknowledge the financial support by self-determined research funds of CCNU from the colleges' basic research and operation of MOE (CCNU15A05020) and National Natural Science Foundation of China (21575047, 21275062).

This work was partly supported by the Centers for Disease Control and Prevention/National Institute for Occupational Safety and Health (CDC/NIOSH) Grant number R21OH010768. The contents of this publication are solely the responsibility of the authors and do not necessarily represent the official views of the CDC.

### References

1. Guo JX, Wu JJQ, Wright JB, Lushington GH. Chem. Res. Toxicol. 2006; 19:209–216. [PubMed: 16485896]

2. Pardo VT, Ibarra N, Rodriguez MA, Waliszewski KN. *J. Agric. Food Chem.* 2001; 49:6057–6062. [PubMed: 11743808]
3. Mercey G, Verdelet T, Renou J, Kliachyna M, Baati R, Nachon F, Jean L, Renard PY. *Acc. Chem. Res.* 2012; 45:756–766. [PubMed: 22360473]
4. Liu GD, Wang J, Barry R, Petersen C, Timchalk C, Gassman PL, Lin YH. *Chem. Eur. J.* 2008; 14:9951–9959. [PubMed: 18942695]
5. Zhang WY, Asiri AM, Liu DL, Du D, Lin YH. *Trends Anal. Chem.* 2014; 54:1–10.
6. Fidder A, Hulst AG, Noort D, Ruiter RD, van der Schans MJ, Benschop P, Langenberg JP. *Chem. Res. Toxicol.* 2002; 15:582–590. [PubMed: 11952345]
7. Hernandez F, Sancho JV, Pozo OJ. *Anal. Bioanal. Chem.* 2005; 382:934–946. [PubMed: 15915347]
8. Sporty SJLS, Lemire SW, Jakubowski EM, Renner JA, Evans RA, Williams RF, Schmidt JG, van der Schans MJ, Noort D, Johnson RC. *Anal. Chem.* 2010; 82:6593–6600. [PubMed: 20617824]
9. Noort D, Fidder A, van der Schans MJ, Hulst AG. *Anal. Chem.* 2006; 78:6640–6644. [PubMed: 16970345]
10. Zhu CZ, Yang GH, Li H, Du D, Lin YH. *Anal. Chem.* 2015; 87:230–249. [PubMed: 25354297]
11. Zhu CZ, Du D, Eychmuller A, Lin YH. *Chem. Rev.* 2015; 115:8896–8943. [PubMed: 26181885]
12. Liu JM, Li Y, Jiang Y, Yan XP. *J. Proteome Res.* 2010; 9:3545–3550. [PubMed: 20450228]
13. Liu R, Liu X, Tang YR, Wu L, Hou XD, Lv Y. *Anal. Chem.* 2011; 83:2330–2336. [PubMed: 21348438]
14. Hansen JA, Wang J, Kawde A, Xiang Y, Gothelf KV, Collins G. *J. Am. Chem. Soc.* 2006; 128:2228–2229. [PubMed: 16478173]
15. Chen BB, Peng HY, Zheng F, Hu B, He M, Zhao W, Pang DW. *J. Anal. Atom. Spectrom.* 2010; 25:1674–1681.
16. Liu GD, Lin YH. *J. Am. Chem. Soc.* 2007; 129:10394–10401. [PubMed: 17676734]
17. Liu GD, Lin YH. *Talanta.* 2007; 74:308–317. [PubMed: 18371644]
18. Lin X, Xie J, Niu G, Zhang F, Gao H, Yang M, Quan Q, Aronova MA, Zhang G, Lee S, Leapman R, Chen XY. *Nano Lett.* 2011; 11:814–819. [PubMed: 21210706]
19. Iwahori K, Yoshizawa K, Muraoka M, Yamashita I. *Inorg. Chem.* 2005; 44:6393–6400. [PubMed: 16124819]
20. MaHam A, Tang ZW, Wu H, Wang J, Lin YH. *Small.* 2009; 5:1706–1721. [PubMed: 19572330]
21. Liu GD, Wu H, Dohnalkova A, Lin YH. *Anal. Chem.* 2007; 79:5614–5619. [PubMed: 17600385]
22. Zhang YY, Tang ZW, Wang J, Wu H, Lin CT, Lin YH. *J. Mater. Chem.* 2011; 21:17468–17475.
23. Liu GD, Wu H, Wang J, Lin YH. *Small.* 2006; 2:1139–1143. [PubMed: 17193578]
24. Du D, Chen AQ, Xie YY, Zhang AD, Lin YH. *Biosens. Bioelectron.* 2011; 26:3857–3863. [PubMed: 21481580]
25. Chen AQ, Bao YW, Ge XX, Shin YS, Du D, Lin YH. *RSC Adv.* 2012; 2:11029–11034.
26. Hsieh HC, Sheu C, Shi FK, Li DT. *J. Chromatogr. A.* 2007; 1165:128–135. [PubMed: 17714720]
27. Li Y, Xu X, Qi D, Deng CH, Yang PY, Zhang XX. *J. Proteome Res.* 2008; 7:2526–2538. [PubMed: 18473453]
28. Chen CT, Chen YC. *Anal. Chem.* 2005; 77:5912–5919. [PubMed: 16159121]
29. Liu GD, Lin YH. *Anal. Chem.* 2005; 77:5894–5901. [PubMed: 16159119]
30. Ge XX, Zhang WY, Du D, Lin YH. *Biosens. Bioelectron.* 2013; 50:486–491. [PubMed: 23911770]
31. Zhang X, Wang HB, Yang CM, Du D, Lin YH. *Biosens. Bioelectron.* 2013; 41:669–674. [PubMed: 23122753]
32. Haigha JR, Lefkowitz LJ, Capacio BR, Doctor BP, Gordon RK. *Chem. Biol. Interact.* 2008; 175:417–420. [PubMed: 18555983]
33. Smith PK, Krohn RI, Hermanson GT, Mallia AK, Gartner FH, Provenzano MD, Fujimoto EK, Goeke NM, Olson BJ, Klenk DC. *Anal. Biochem.* 1985; 150:76–85. [PubMed: 3843705]
34. Guesdon JL, Ternynck T, Avrameas S. *J. Histochem. Cytochem.* 1979; 27:1131–1139. [PubMed: 90074]



35. Nawrocki J, Dunlap C, McCormick A, Carr PW. J. Chromatogr. A. 2004; 1028:1–30. [PubMed: 14969280]

Author Manuscript

Author Manuscript

Author Manuscript

Author Manuscript

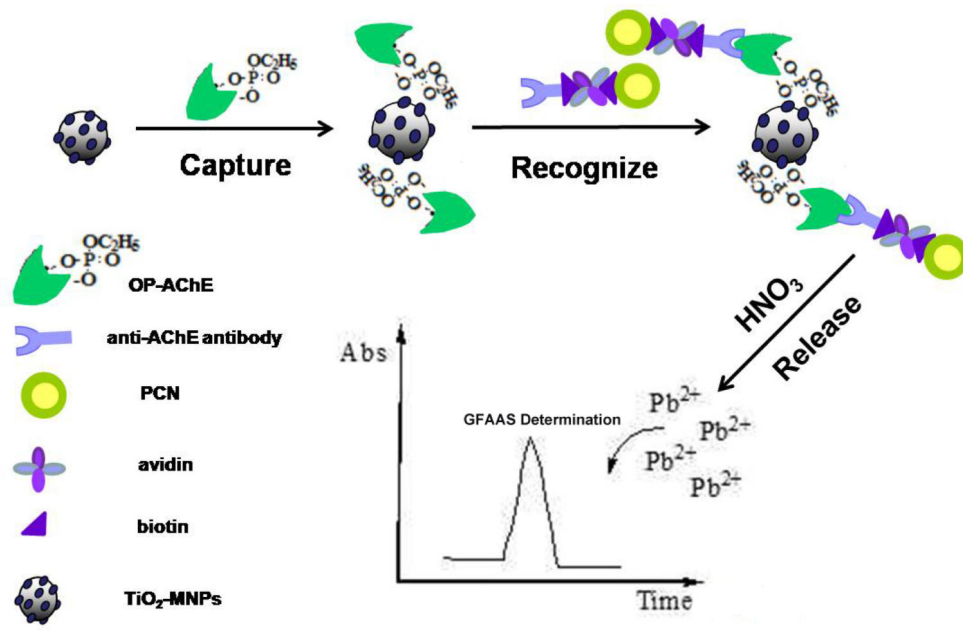


**Fig. 1.**  
Schematic illustration of the sandwich-like immunoassay of OP-AChE adducts

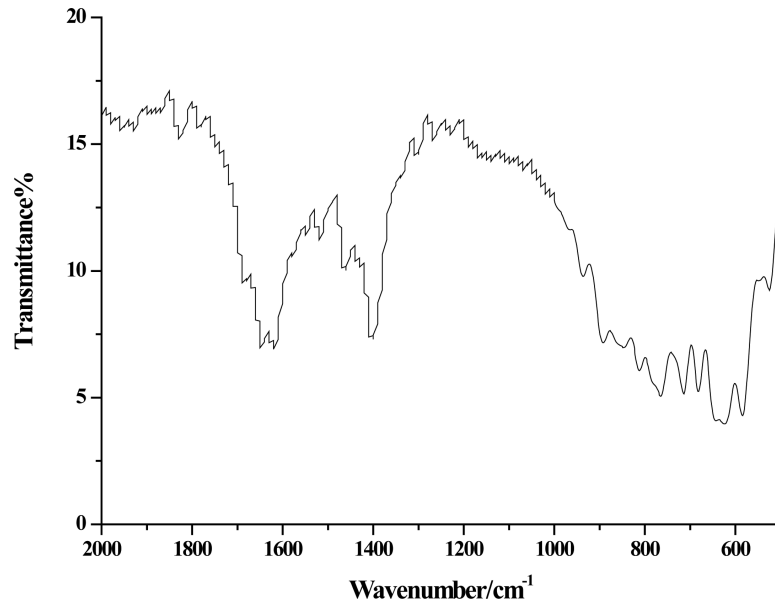


**Fig. 2.**  
FTIR spectrum of OP-AChE adduct

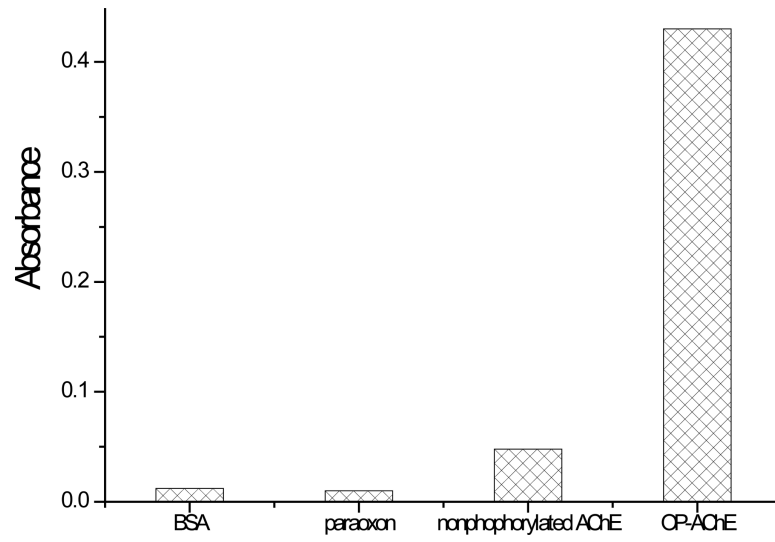


**Fig. 3.** GFAAS responses of the immunoassay for OP-AChE, nonphosphorylated AChE, paraoxon and BSA

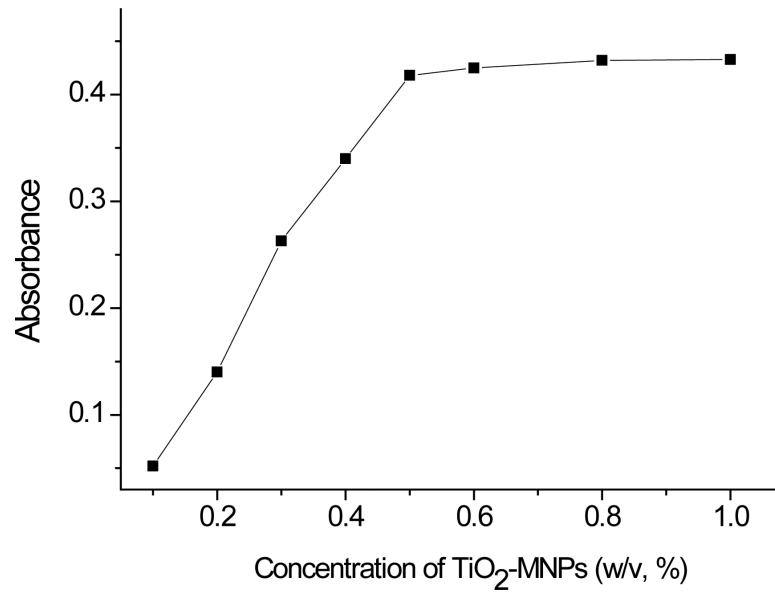


**Fig. 4.** Effect of the amount of TiO<sub>2</sub>-MNPs on the immunoassay responses

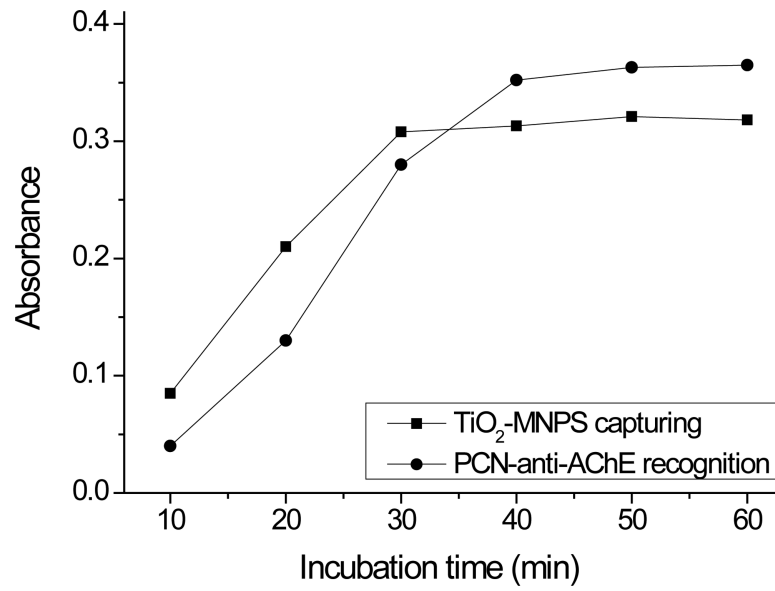


**Fig. 5.**  
Effect of the incubation time on the immunoassay responses

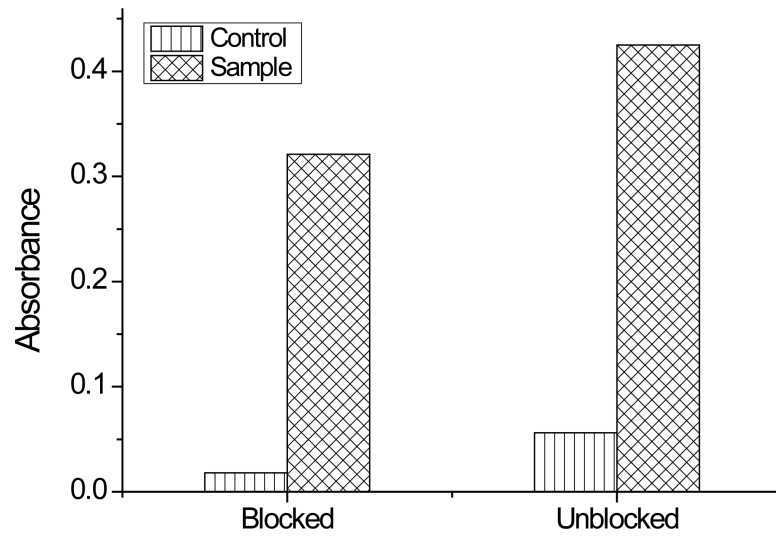


**Fig. 6.**  
Effect of the non-specific adsorption on the immunoassay responses

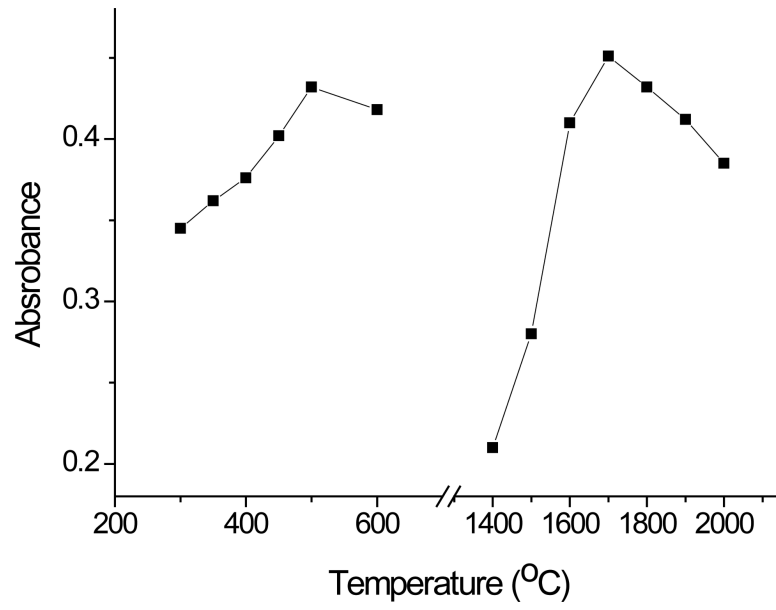


**Fig. 7.**  
Pyrolysis curve and atomization curve for Pb



**Table 1**

## Operating parameters for GFAAS

Parameters	
Lamp current (mA)	2.0
Wavelength (nm)	283.3
Slit (nm)	0.4
Ar flow rate (mL min <sup>-1</sup> )	300 (stopped during atomizing)
Sample volume (μL)	10

Temperature program	
Drying	110 °C (Ramp 18s, Hold 10s)
Pyrolysis	500 °C (Ramp 10s, Hold 10s)
Atomization	1700 °C (Ramp 0s, Hold 4s)
Cleaning	2000 °C (Ramp 1s, Hold 3s)

**Table 2**

Analytical results for the spiked human plasma samples with immunoassay (n=3)

<b>Sample No.</b>	<b>1</b>	<b>2</b>	<b>3</b>	<b>4</b>	<b>5</b>	<b>6</b>
Add (nM)	0	0.02	0.05	0.10	0.50	1.00
Found (nM)	nd	0.021	0.047	0.976	0.518	1.018
Recovery (%)	--	105	94	97.6	103.6	101.8

nd: no detected

Author Manuscript

Author Manuscript

Author Manuscript

Author Manuscript